

## Study of the photovoltaic properties of GaPN(As) heterostructures on silicon substrates

© E.V. Nikitina<sup>1,2</sup>, A.K. Kaveev<sup>1</sup>, V.V. Fedorov<sup>2</sup>, O.A. Sinititskaya<sup>2</sup>, S.N. Khrul<sup>2</sup>, G.E. Yakovlev<sup>3</sup>,  
A.S. Gudovskikh<sup>2</sup>

<sup>1</sup> Ioffe Institute, St. Petersburg, Russia

<sup>2</sup> Alferov Federal State Budgetary Institution of Higher Education and Science Saint Petersburg National Research Academic University of the Russian Academy of Sciences, St. Petersburg, Russia

<sup>3</sup> St. Petersburg State Electrotechnical University LETI, St. Petersburg, Russia

E-mail: mail.nikitina@mail.ru

Received December 1, 2025

Revised December 11, 2025

Accepted December 11, 2025

This paper presents studies of photovoltaic properties of  $p-i-n$  heterostructures based on solid solutions GaPN and GaPNAs, which were grown on silicon substrates. Studies of current-voltage characteristics and external quantum efficiency spectra have demonstrated that structures based on quadruple solid solutions GaPNAs have a greater potential compared to triple solid solutions GaPN that do not contain arsenic. For the GaPNAs-based structures, despite a narrower bandgap, a higher open-circuit voltage (0.78 V) was achieved compared to  $p-i-n$  GaPN heterostructures, which indicates a lower defect concentration in the GaPNAs layers.

**Keywords:** dilute nitrides, GaPN(As) on a silicon substrate,  $p-i-n$  heterostructures.

DOI: 10.61011/TPL.2026.04.63205.20585

The procedure for creating silicon solar cells is well developed; however, their efficiency is at present limited to 26% and is very close to its theoretical limit [1]. The need to create cheap, compact, and highly efficient sources of renewable energy prompts researchers to examine the possibility of creating monolithic multi-junction solar cells on silicon substrates. Creation of such a device is prevented by the lack of a proven procedure for fabricating semiconductor materials lattice-matched to a silicon substrate. Among the materials able to be used in the upper cascades of solar cells with silicon-based lower cascades, there are GaPN and/or GaPNAs with the nitrogen content of several percent. Using these materials, it is possible to achieve lattice matching with silicon; in this case, the bandgap width will be 1.5–2.0 eV. Papers [2,3] have shown theoretically the GaPN(As) potential as upper junctions for solar cells monolithically integrated on silicon substrates; however, despite the theoretical possibility of using this material in photovoltaics, growing „diluted nitrides“ is a complex task, and large number of defects in the resulting heterostructures prevents achieving the theoretically predicted results [4,5].

The GaPN and GaPNAs photoconverting structures considered in this study were grown by molecular beam epitaxy on  $n$ -Si (001) substrates with the [011] misorientation of  $4^\circ$  by using setup Veeco Gen III with a plasma source of nitrogen; the substrate resistivity was 0.01–0.02  $\Omega \cdot \text{cm}$ .

Structures Nos 1 and 2 considered in this study are  $p-i-n$  heterostructures with undoped GaPN layers 300 and 600 nm thick, respectively, enclosed between the  $p$ - and  $n$ -doped GaP layers 100 nm thick each. In addition, the  $n$ -GaP layer partially served as a buffer layer between the

heterostructure and silicon substrate; its growth temperature was initially 450 °C and increased gradually to 600 °C. Doping levels of  $p$  and  $n$  GaP were  $(0.8-1.0) \cdot 10^{19} \text{ cm}^{-3}$  and  $(4-5) \cdot 10^{17} \text{ cm}^{-3}$ , respectively.

Structure No 3 was also a  $p-i-n$  heterostructure with undoped GaPNAs layer 200 nm thick sandwiched between the  $p$ - and  $n$ -doped GaPNAs layers 500 nm thick each. Between the silicon substrate and GaPNAs layers there was a 50 nm thick  $n$ -GaP buffer layer grown under a gradient temperature increase from 450 to 600 °C. A 40 nm thick  $p$  GaP layer was grown on top of the GaPNAs layer. Doping levels of the  $p$  and  $n$  layers were preset to the same value as for the  $p-i-n$  GaPN samples.

The back contact to the silicon substrate was formed using indium, that on  $p$  GaP was created by vacuum deposition through a mask of Ni/Au layers 10 and 100 nm in thickness, respectively, with annealing at 400 °C for 1 min.

Fig. 1 presents I-V characteristics of the studied  $p-i-n$  GaPN structures (samples Nos 1 and 2) without illumination and under illumination by a solar radiation simulator with the AM1.5G spectrum ( $100 \text{ mW/cm}^2$ ). The main photovoltaic characteristics of the grown heterostructures are given in the Table.

Comparison of I-V characteristics of samples with different thicknesses of the  $i$ -GaPN layer shows that the sample of a greater thickness exhibits under illumination lower values of both short-circuit current and open-circuit voltage. This behavior of the I-V characteristic may be associated with an increase in the number of defects in the  $i$ -GaPN layer with increasing pseudomorphic layer thickness. This type of dependence may also be explained by the fact that, as

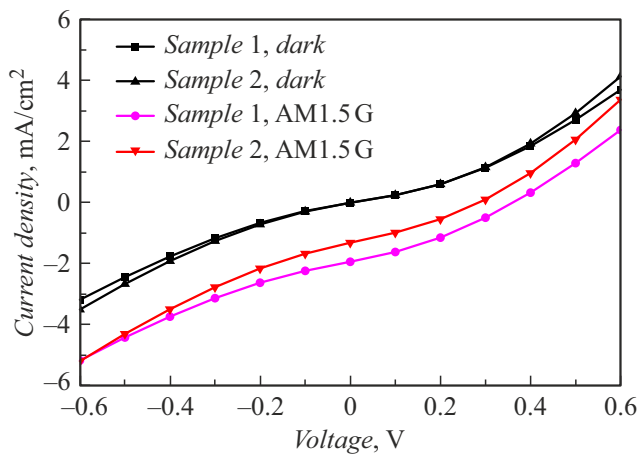


**Figure 1.** I-V characteristics of  $p-i-n$  heterostructures with an  $i$  GaPN layer 300 nm thick (sample No 1) and 600 nm thick (sample No 2) without illumination (*dark*) and with illumination (AM1.5G).

the  $i$ -GaPN layer thickness increases, there takes place a decrease in the electric field promoting the charge carrier separation and preventing their recombination. Hence, the increase in recombination losses leads to a decrease in short-circuit current and open-circuit voltage.

Growth of recombination losses with increasing  $i$ -GaPN layer thickness from 300 to 600 nm is also manifested by the shape of external quantum efficiency (EQE) spectra presented in Fig. 2. On the one hand, with increasing thickness an expected increase in EQE proceeds in the long-wave range, which is caused by an increase in the number of absorbed photons in this spectrum range. On the other hand, a significant decrease in EQE is observed in the short-wave range and maximum-sensitivity range, which is typical for recombination losses in the  $i$ -region of  $p-i-n$  structures.

High defect concentration in these structures is also evidenced by high leakage currents at negative voltages. As shown by dark I-V characteristics (Fig. 1), a sharp increase in dark current is observed with increasing reverse voltage, which is apparently caused by recombination losses. For the reverse voltage, the I-V characteristic shapes in the dark and under illumination are almost the same for both structures and differ only in the photocurrent magnitude which is practically independent of the reverse voltage. However, while the forward bias voltage increases,

a decrease in photocurrent is observed; this decrease is most pronounced for the structure with a thicker  $i$  GaPN layer. This difference also indicates high defect concentration in the  $i$  region. An increase in forward voltage promotes reduction in electric field in the  $i$  GaPN layer and, hence, leads to an increase in recombination losses. Paper [6] demonstrates a significant decrease in photocurrent with increasing forward voltage under an increase in defect concentration in the  $i$  region of  $p-i-n$  structures.

I-V characteristics of the  $p-i-n$  GaPNAs-structure (sample No 3) with and without AM1.5G illumination are shown in Fig. 3. The I-V characteristic shapes manifest a significantly lower leakage current in this structure than in  $p-i-n$  heterostructures with the  $i$  GaPN layer. In addition, the  $p-i-n$  GaPNAs heterostructure exhibits open-circuit voltage (0.78 V) significantly higher than that for  $p-i-n$  GaPN heterostructures, despite a narrower GaPNAs bandgap. The decrease in the GaPNAs bandgap width is evidenced by the absorption edge shift to the long-wave range observed in the EQE spectra (Fig. 2). These facts in combination indicate for the GaPNAs heterostructure significantly lower recombination losses and lower defect concentration compared to those for GaPN-based structures.

Gentle slope of the dark I-V characteristic forward branch (Fig. 3) is due to the influence of series resistance. Forward branch of the illuminated I-V characteristic has a steeper slope and intersects with the dark I-V characteristic. This behavior of the I-V characteristics indicates a series resistance decrease due to illumination-induced generation of nonequilibrium carriers, which can either increase the conductivity of an insufficiently doped layer or lead to a decrease in band bending at the heterointerface.

The assumption about insufficient doping of the  $p-i-n$  GaPNAs heterostructure (sample No 3), which was made based on the I-V characteristic behavior, has been also confirmed by numerical simulation performed using code AFORS-HET v2.4.1. In the case of heavy doping ( $> 10^{17} \text{ cm}^{-3}$ ) of the  $p$  GaPNAs layer, most of the charge carriers generated in this 500 nm thick layer recombine since the layer is almost fully free of electric field. This results in a quite narrow EQE spectrum with the maximum at about 600 nm. If the doping level is  $\leq 10^{15} \text{ cm}^{-3}$ , band bending extends over a larger part of the layer thickness, which promotes reduction of recombination losses and, hence, makes the EQE spectrum broader than that observed

Main photovoltaic characteristics of the  $p-i-n$  GaPN and GaPNAs heterostructures grown on silicon substrates under AM1.5G solar radiation ( $100 \text{ mW/cm}^2$ )

Sample No	Brief description of the heterostructure	Open-circuit voltage, V	Short-circuit current density, $\text{mA/cm}^2$	Occupation coefficient ( $FF$ ), %
1	$p-i-n$ GaPN, 300 nm $i$ -GaPN	0.28	1.3	31.4
2	$p-i-n$ GaPN, 600 nm $i$ -GaPN	0.36	2.0	32.5
3	$p-i-n$ GaPNAs	0.78	1.3	36.3

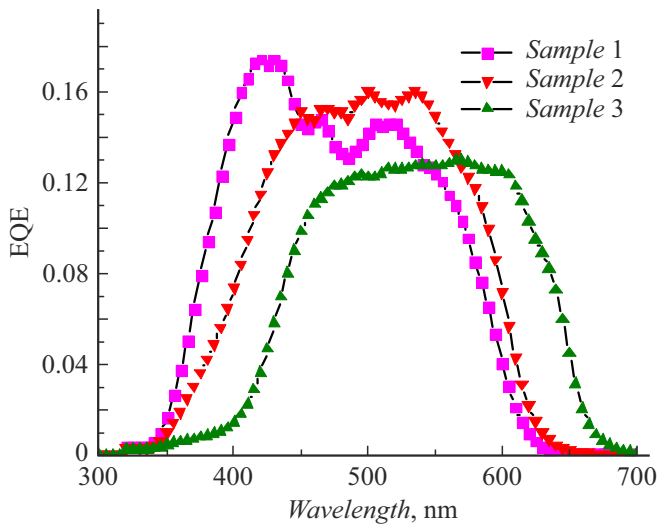


**Figure 2.** External quantum efficiency (EQE) spectra of  $p-i-n$  heterostructures.

experimentally. In addition, the dopant profile was studied using electrochemical capacitance-voltage profiling (ECV). Fig. 4 presents the doping profile for the  $p-i-n$  GaPNAs heterostructure (sample No 3). One can see that on the heterostructure front side only the  $p$  GaP layer (40 nm) exhibits a considerable doping level ( $> 10^{18} \text{ cm}^{-3}$ ). Doping level of the  $p$  GaPNAs layer is impossible to be determined; what is only possible is to estimate it as not exceeding  $10^{17} \text{ cm}^{-3}$ . Thus, we may unambiguously state that doping of the  $p$  GaPNAs layer appears to be insufficient to form the  $p-i-n$  structure cladding.

Studies presented in this paper have shown that adding arsenic to the GaPN solid solution, i.e. using the GaPNAs solid solution, may improve characteristics of  $p-i-n$  heterostructures. However, the structure design needs more investigation aimed at increasing the external quantum efficiency of the dilute-nitride-based photoconverter

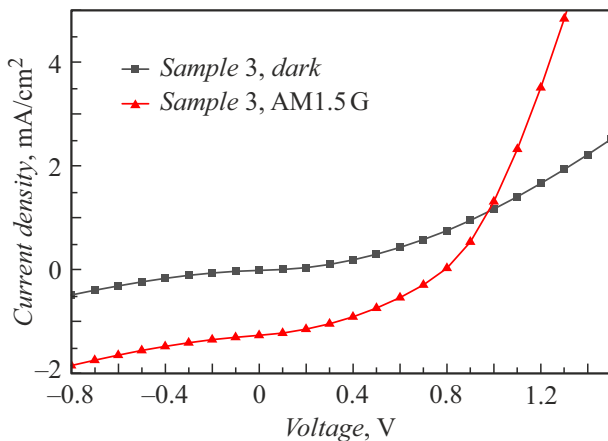


**Figure 3.** I-V characteristics of the  $p-i-n$  heterostructure with the  $i$  GaPNAs layer (sample No 3) without illumination (*dark*) and under illumination (AM1.5G).

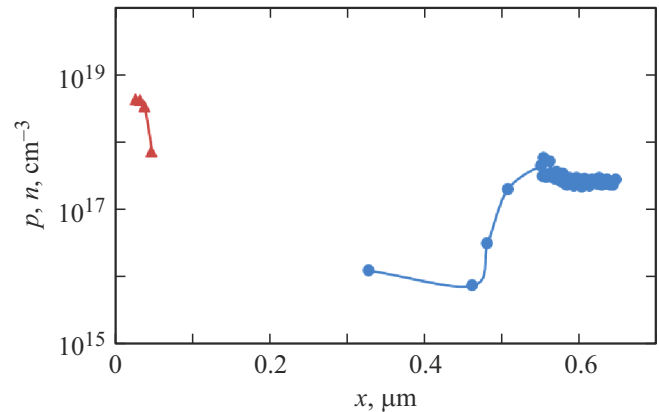


**Figure 4.** Doping profile in the  $p-i-n$  GaPNAs-heterostructure (sample No 3).

heterostructure fabricated by molecular beam epitaxy on a silicon substrate.

### Funding

The study was supported by the Russian Science Foundation grant No 23-79-00032 (<https://rscf.ru/project/23-79-00032/>).

### Conflict of interests

The authors declare that they have no conflict of interests.

### References

- [1] A. Richter, R. Müller, J. Benick, F. Feldmann, B. Steinhauser, Ch. Reichel, A. Fell, M. Bivour, M. Hermle, S.W. Glunz, *Nat. Energy* **6**, (2021). DOI: 10.1038/s41560-021-00805-w
- [2] J.F. Geisz, D.J. Friedman, *Semicond. Sci. Technol.*, **17** (8), 769 (2002). DOI: 10.1088/0268-1242/17/8/305
- [3] D.A. Kudryashov, A.S. Gudovskikh, E.V. Nikitina, A.Yu. Egorov, *Semiconductors*, **48** (3), 381 (2014). DOI: 10.1134/S1063782614030154.
- [4] A. Baranov, A. Gudovskikh, A.Yu. Egorov, D. Kudryashov, S. Le Gall, J.-P. Kleider, *J. Appl. Phys.*, **128**, 023105 (2020). DOI: 10.1063/1.5134681
- [5] L.N. Dvoretckaia, A.D. Bolshakov, A.M. Mozharov, M.S. Sobolev, D.A. Kirilenko, A.I. Baranov, V.Yu. Mikhailovskii, V.V. Neplokh, I.A. Morozov, V.V. Fedorov, I.S. Mukhin, *Solar Energy Mater. Solar Cells*, **206**, 110282 (2020). DOI: 10.1016/j.solmat.2019.110282
- [6] A.S. Gudovskikh, A.S. Abramov, A.V. Bobyl, K.S. Zelentsov, D.A. Kudryashov, I.A. Morozov, E.I. Terukov, D.L. Orehov, V.N. Verbitskiy, in *Proc. of the 28th European Photovoltaic Solar Energy Conf. and Exhibition* (Paris, France, 2013), p. 2495.

Translated by EgoTranslating